Superconductivity and electron-phonon coupling in lithium at high pressures

Timur Bazhirov, Jesse Noffsinger, and Marvin L. Cohen
Department of Physics, University of California at Berkeley, Berkeley, California 94720, USA
and Materials Sciences Division, Lawrence Berkeley National Laboratory, Berkeley, California 94720, USA
(Received 11 August 2010; published 8 November 2010)

Using a first-principles pseudopotential approach we study the origin of superconductivity in lithium under pressure. A recently developed Wannier interpolation based technique that allows for ultradense sampling of electron-phonon parameters throughout the Brillouin zone was employed. The electron-phonon coupling strength as a function of pressure was calculated, precisely resolving many of the fine features of its distribution. The contributions to coupling arising from the Fermi surface topology, phonon dispersions, and electron-phonon matrix elements were separately analyzed. It is found that of the constituent components, the electron-phonon matrix elements are the most sensitive to pressure changes, and a particular phonon is responsible for high values of coupling. Additionally, the distribution of matrix elements over the Fermi surface is seen to be non-uniform and possesses a two-peak structure. Analysis of the Eliashberg spectral function $\alpha^2F(\omega)$ shows a considerable increase in spectral weight in the low-frequency region with the application of pressure. We estimate the superconducting transition temperature and find that the obtained values are in good accord with experiment.

DOI: 10.1103/PhysRevB.82.184509 PACS number(s): 74.25.Kc, 74.25.Dw, 74.62.Fj

I. INTRODUCTION

Lithium has attracted particular attention because it is a simple metal that exhibits a complex phase diagram. At ambient conditions it is a very nearly free-electron bcc metal[1] and its Fermi surface shows little deviation from a sphere. It may be expected that lithium would become more free-electron-like with pressure increase. Experiments show, however, that when temperature is decreased or pressure is applied, Li undergoes several structural transitions and becomes superconducting.[2–7]

In the bcc structure at atmospheric pressure, it has been found that the superconducting phase transition occurs at temperatures below the millikelvin range.[2] The presence of a bcc to 9*R* phase transition near 80 K indicates that the zero-pressure superconducting structure is likely not bcc.[3,8] For nonzero pressures, Li begins to show superconductivity at pressures near 20 GPa in the fcc phase and exhibits a maximum transition temperature of 14 K at 30 GPa,[5–7] making it among the highest T_c elemental superconductors. Further pressure increases beyond 30 GPa lead to structural transitions which lower T_c.[9] Additionally it was recently shown that at around 70 GPa, Li undergoes a metal-to-insulator transition[10] while resistivity increases with pressure have also been observed for shock-wave experiments.[11]

Previous theoretical studies indicate that the electron-phonon coupling strength in lithium is substantial.[12–17] A large electron-phonon coupling strength for the bcc structure was first calculated from the empirical pseudopotential method and then in a first-principles pseudopotential approach[12,13] while the total electron-phonon couplings in both bcc and fcc phases has been previously analyzed. Significantly higher superconducting transition temperatures than experimentally observed have been predicted using the calculated coupling strengths for multiple structures of Li.[14] It was found that the Fermi surface topology plays a crucial role in the onset of superconductivity. Unlike the case of bcc Li, Fermi surface nesting appears to be important in the fcc phase. Several features which include phonon softening with pressure, a peak in the nesting function near the Brillouin zone (BZ) edge and strong coupling to specific phonons have been suggested as the origin of superconductivity in Li under pressure.[15,16] In previous electron-phonon reports it has been suggested that a very fine BZ sampling is necessary to calculate the total coupling parameters in pressurized Li with high precision.[15–18] Interestingly, studies under extreme pressures indicate that the electronic structure of Li evolves into a paired insulating state which gives an upper limit to the pressure at which superconductivity may be observed.[10,19]

In this paper we study the pressure evolution of the total electron-phonon coupling for the monatomic fcc phase of Li in the 8–36 GPa range. Applying a method based on first-principles calculations and subsequent Wannier interpolation techniques, we have resolved the fine features of the coupling strength λ throughout the BZ. We analyze λ in terms of the effective contributions from three different terms: Fermi surface nesting, phonon frequencies, and electron-phonon matrix elements. The Eliashberg spectral function $\alpha^2F(\omega)$ is obtained and the superconducting transition temperature is calculated through the modified McMillan equation.[20] We also discuss the possibility of routes to higher T_c.

II. METHODOLOGY

A. Electron-phonon coupling and superconductivity

In this work, we study the wave-vector specific coupling parameter $\lambda_{\vec{Q},\nu}$ within the isotropic Migdal approximation.[21–23] The electron-phonon coupling strength is calculated for a particular wave vector $\vec{Q}$ inside the BZ and mode index ν as

$$\lambda_{\vec{Q},\nu} = \frac{2}{N(0)\omega_{\vec{Q},\nu}} \frac{1}{N} \sum_{\vec{k}} |M^{[\nu]}_{\vec{k},\vec{k}+\vec{Q}}|^2 \delta(\epsilon_{\vec{k}}) \delta(\epsilon_{\vec{k}+\vec{Q}}), \quad (1)$$

where $M^{[\nu]}_{\vec{k},\vec{k}+\vec{Q}}$ is the electron-phonon matrix element, $\omega_{\vec{Q},\nu}$ the phonon frequency, $N(0)$ the density of states at the Fermi level, and $\delta(\epsilon_{\vec{k}})$ the energy-conserving delta function. We can divide Eq. (1) into three main components. The first one being the Fermi surface nesting function $\xi_{\vec{Q}}$,

$$\xi_{\vec{Q}} = \frac{1}{N} \sum_{\vec{k}} \delta(\epsilon_{\vec{k}}) \delta(\epsilon_{\vec{k}+\vec{Q}}). \quad (2)$$

The nesting function is a geometrical property of the Fermi surface and is particularly large for wave vectors which connect parallel portions of the surface. The second contribution arises from the phonon eigenfrequncy $\omega_{\vec{Q},\nu}$, which can be affected by the application of pressure not only by an overall change in the lattice spring constant, but also through the appearance of Kohn anomalies. The final component, which contributes to the electron-phonon coupling strength, is the matrix element $M^{[\nu]}_{\vec{k},\vec{k}+\vec{Q}}$, which accounts for the details of the interaction between electronic eigenstates and lattice vibration. The matrix element can be expressed as

$$M^{[\nu]}_{\vec{k},\vec{k}+\vec{Q}} = \left(\frac{\hbar}{m\omega_{\vec{Q},\nu}} \right)^{1/2} \langle \vec{k} | \delta_\nu V | \vec{k} + \vec{Q} \rangle, \quad (3)$$

where $\delta_\nu V$ is the phonon perturbation for a particular mode and $\langle \vec{k}|$ is the Kohn-Sham electronic eigenstate. Band indices have been omitted for clarity. The Eliashberg spectral function can be obtained through a BZ integral of $\lambda_{\vec{Q},\nu}$ as

$$\alpha^2 F(\omega) = \frac{1}{2N} \sum_{\vec{Q},\nu} \omega_{\vec{Q},\nu} \lambda_{\vec{Q},\nu} \delta(\omega - \omega_{\vec{Q},\nu}). \quad (4)$$

Then we extract the frequency moments of the spectral function and use the average coupling

$$\lambda = 2 \int \omega^{-1} \alpha^2 F(\omega) d\omega = 1/N \sum_{\vec{Q},\nu} \lambda_{\vec{Q},\nu} \quad (5)$$

in the modified McMillan equation[20] to estimate the superconducting transition temperature T_c.

B. Computational details

The electronic structure was calculated using the local-density approximation (LDA) to density-functional theory[24,25] within a plane-wave pseudopotential scheme.[26] The norm-conserving Li pseudopotential included $2s$ and $2p$ states in the valence and a nonlinear core correction. The pseudopotential was generated according to the Troullier-Martins scheme.[27] A 30 Ry kinetic-energy cutoff was enough to attain convergence for total-energy calculations. We did not include the $1s$ valence state as it introduced the need for a much higher kinetic-energy cutoff without significantly increasing the precision of the calculations.[19] The pseudopotential cutoff radius of 2.5 a.u. was small enough to avoid core overlap up to the pressures studied in this work.

Lattice dynamical properties were obtained through density-functional perturbation theory[28] and the electron-phonon coupling matrix elements and total coupling parameter were calculated using a first-principles interpolation scheme[29] based on maximally localized Wannier functions.[29–32] An $8 \times 8 \times 8$ initial sampling of the Brillouin zone was suitable to achieve an acceptable real-space decay necessary for convergence of both the interpolated electronic structure and lattice dynamics. The final sampling of the BZ was performed on a momentum space grid containing as many as 8 million wave vectors.

III. RESULTS

The results presented here are for fcc Li at five pressures: 8, 14, 20, 30, and 36 GPa. The relative compressions corresponding to these pressures are 0.73, 0.64, 0.57, 0.51, and 0.48, respectively. Using the generated pseudopotential, we find good agreement with the room-temperature experimental equation of state[4] and slope $\frac{\delta P}{\delta V}$. It is well known that LDA slightly underestimates equilibrium bond lengths and for a given value of atomic volume the experimental pressure is about 2 GPa higher than our LDA value. The pressures listed here are those from LDA calculation.

There exists a widely accepted consensus that Li is an electron-phonon superconductor, so one should expect that the experimental rise in superconducting transition temperature would arise from an increase in electron-phonon coupling. Following the decomposition of $\lambda_{\vec{Q},\nu}$ into the three primary contributions, we start by analyzing how pressure affects the Fermi surface nesting function $\xi_{\vec{Q}}$. From Fig. 1(a) it can be seen that although pressure does affect $\xi_{\vec{Q}}$, the nesting function is in general suppressed as pressure increases. This is true for nearly all Q vectors inside the BZ with the exception of a small region around the K point which shows a definite increase in the Fermi surface nesting function. This increase alone is clearly not enough to account for the experimental rise in T_c seen with the application of pressure. Therefore, we conclude that the nesting function which does not vary strongly with pressure does not contribute significantly to the increase in $\lambda_{\vec{Q},\nu}$.

We have calculated that most of the electron-phonon coupling strength in Li comes from the lower transverse mode $T1$. Therefore, we concentrate our analysis on this particular phonon mode. From Fig. 1(b) we see that a softening of phonon frequencies is present around the L point of the BZ, and a more significant softening occurs along the Γ-K direction. From Eq. (1) the coupling is expected to increase as phonon frequencies are softened. Indeed, this is visible in Fig. 1(d). An examination of the softening of $\omega_{\vec{Q}}$ near the symmetry point K leads to the conclusion that a simple scaling of lambda by the frequency cannot completely account for the large increase in coupling found in this part of the BZ. On the other hand, the response of the average matrix elements to pressure in Fig. 1(c) is very similar to that of the wave-vector-dependent coupling in Fig. 1(d). Both show sharp increase with pressure near K.

An analysis of $M^{[\nu]}_{\vec{k},\vec{k}+\vec{Q}}$ can be performed by looking at the distribution of the magnitudes of the matrix elements over

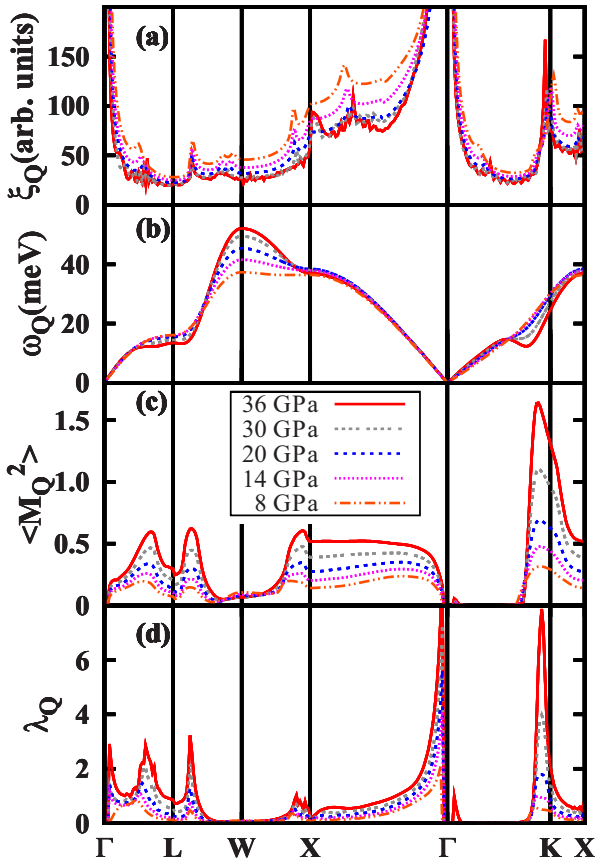

FIG. 1. (Color online) (a) The Fermi surface nesting function $\xi_{\vec{Q}}$, (b) phonon dispersions $\omega_{\vec{Q}}$, (c) average matrix element squared $M^2_{\vec{Q}}$, and (d) electron-phonon coupling $\lambda_{\vec{Q}}$ for fcc Li along the path inside the Brillouin zone. (b)–(d) are given for lower transverse mode $T1$. In (c) the dimensions of matrix elements are $meV^2 \times 10^3$.

the BZ. Since the matrix elements depend on both $\vec{Q}$ and $\vec{k}$, we examine $\vec{Q}_0=(0.6,0.6,0.0)$, which is close to the peak of the $\lambda_{\vec{Q}}$ with pressure. We calculate $M=M^{[T1]}_{\vec{k},\vec{k}+\vec{Q}_0}$ on a $200\times200\times200$ k-point mesh in the BZ and filter only k states with energy close to the Fermi level. The distribution of the matrix elements shown in Fig. 2 has a two-peak structure where a small portion of the matrix elements have values more than an order of magnitude larger than the rest. This structure persists at all pressures but the size of the matrix elements is affected strongly as pressure is increased. For higher pressures the fraction of elevated electron-phonon matrix elements is smaller but the magnitudes of these matrix elements are increased. The regions of Fermi surface where M^2 have the highest values are a small fraction of the BZ. As the pressure increases, these regions become more concentrated.

The Eliashberg spectral function obtained according to Eq. (4) is shown in Fig. 3. For comparison, the phonon density of states is also presented. We see that though the higher frequency LA peak is stiffened with pressure for both $\alpha^2F(\omega)$ and $F(\omega)$ as expected, the behavior of the lower frequency TA peak differs qualitatively between these two graphs. In the $F(\omega)$ graph, the low-frequency peak position

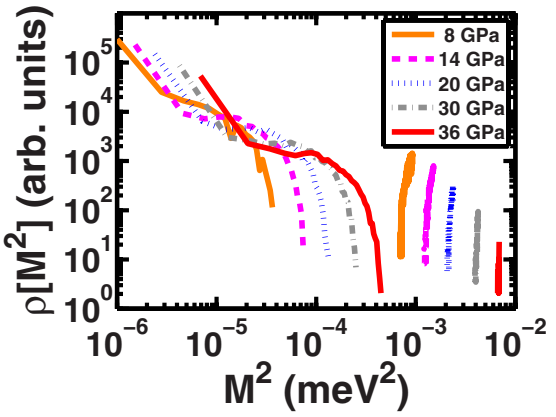

FIG. 2. (Color online) Magnitude density distribution of the electron-phonon matrix elements $M_{\vec{k},\vec{k}+\vec{Q}}$ for the lower transverse mode $T1$ of fcc Li with $\vec{Q}=(0.6,0.6,0.0)$. Only matrix elements for the k states close to Fermi level are included. The magnitude density distribution is a histogram which plots the number of occurrences of a particular matrix element magnitude throughout the Brillouin zone as a function of that magnitude.

varies slightly with pressure while the peak positions coincide in the spectral function, the magnitude of the coupling, $\alpha^2=\alpha^2F/F$ is significantly amplified as pressure is applied. This increased spectral weight in the low-frequency region is primarily responsible for the higher values of average coupling λ. Once again, this observation emphasizes the importance of the coupling matrix elements on the increased transition temperature in Li under pressure.

An enumeration of certain frequency moments of the Eliashberg spectral function and the resulting estimated values of the superconducting transition temperature are given in Table I. The superconducting transition temperature corresponding to the calculated electron-phonon coupling parameter has been obtained using the modified McMillan equation.[20] The total electron-phonon coupling strength λ, logarithmic and average square frequencies[21] $\omega_{\log}$ and $\langle\omega^2\rangle^{1/2}$ are consistent with previous calculations in Refs. 15–18. Be-

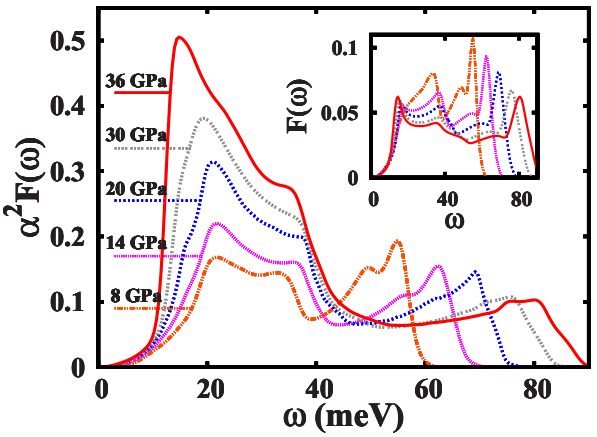

FIG. 3. (Color online) Eliashberg function $\alpha^2F(\omega)$ for different values of pressure. Effective sampling of $50\times50\times50$ k and q points inside the BZ was utilized. (Inset) Phonon densities of states $F(\omega)$ for the same pressures.

TABLE I. Pressure evolution of different order frequency moments of spectral function $\alpha^2F(\omega)$. We show the total coupling strength λ, as well as the logarithmic and square average frequencies (in K). The superconducting transition temperature (T_c, in K) is estimated using the Allen-Dynes formula (Ref. 20) with a Coulomb parameter μ^* given above.

P (GPa)	$\omega_{\log}$	$\langle\omega^2\rangle^{1/2}$	λ	$T_c(\mu^*=0.13)$	$T_c(\mu^*=0.2)$
8	308	378	0.39	0.5	0.01
14	293	376	0.49	2.0	0.3
20	288	373	0.66	6.8	2.7
30	274	360	0.83	12.2	6.8
36	255	341	1.10	20.0	14.2

cause of the ultrafine sampling of the BZ our results are well converged with respect to the summation over the BZ. Small features that were previously difficult to study have been resolved. We see that both logarithmic and square average frequencies decrease monotonically with pressure, arising from the shift of spectral weight to lower frequencies. On the other hand, the average coupling strength λ increases from 0.39 at 8 GPa to 1.10 at 36 GPa, resulting in a dramatic increase in T_c.

The superconducting equation of state for Li is plotted in Fig. 4 where theoretical results from this work are given together with experimental results.[5–7] Good agreement is observed in the region from 20 to 30 GPa where the different experimental results are consistent with each other. Outside of this pressure region, there are some discrepancies among experimental results.

IV. DISCUSSION

It has been suggested that Fermi surface nesting plays crucial role in the onset of superconductivity in fcc lithium.[15] In this work we observe the nesting to be important and indicative of increases in coupling $\lambda_{\vec{Q}}$. However, the change

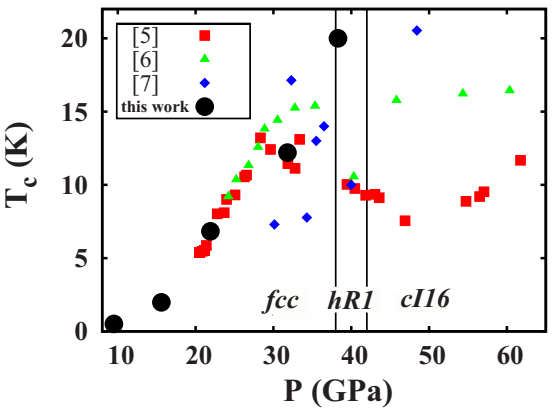

FIG. 4. (Color online) Superconducting temperature vs pressure phase diagram for Li. Experimental data from Refs. 5–7 are shown as well as calculated results based on Allen-Dynes equation with $\mu^*=0.13$. Proposed phase-stability boundaries from Ref. 9 are indicated by vertical lines.

in the nesting function with pressure is seen to be much less than what is necessary to account for the increase in electron-phonon coupling strength evidenced by the increase in the superconducting transition temperature. This suggests that the pressure affects phonons more strongly than it does affect the Fermi surface topology of Li. In other words, it can be said that the Fermi surface topology in the fcc phase creates necessary conditions for superconductivity to appear whereas applying pressure adds coupling strength, thereby driving the transition temperature up.

The origin of increasing electron-phonon interactions can be seen by a large deformation potential caused by particular phonons as shown in our calculations. To understand this, it is worthwhile to consider what happens when Li atoms are pushed close together by pressure. It has been suggested that the high-pressure pairing in lithium results from a redistribution of the charge density.[19] As pressure is applied, the 2s orbitals eventually begin to overlap and at some point the mutual repulsion causes the electrons to occupy more favorable interstitial regions between Li dimers. This is similar to a Peierls'-type transition and could account for the theoretically predicted s-p transition,[15,33] where p-type orbitals lower the total-energy resulting in the appearance of paired-type structures ($cI16$). The paired structures are favorable as they tend to maximize the interstitial volume of the unit cell. If we assume that the described process is smooth, it is natural to suggest that the change in electronic structure with pressure also strongly affects the lattice dynamics. These affected dynamics may be the cause of higher electron-phonon coupling and eventually the structural transition associated with the $T1$ phonon softening. Experimental measurements of the pressure dependence of resistivity show a monotonic continuous trend in the region below 40 GPa.[10] This is consistent with the above assumption of continuous transformation of electronic structure under pressure.

The two-peak structure of the electron-phonon matrix elements indicates that there are areas of BZ which have much stronger coupling matrix elements, differing by an order of magnitude or more. We have studied the magnitude density distribution of $\lambda_{\vec{Q}}$ and observe a structure consistent with the two-peak graph of Fig. 2. The latter distribution has one peak in the low $\lambda_{\vec{Q}}$ region and a second, softer peak in the higher coupling region arising from these stronger matrix elements. Conversely, the same analysis of $\xi_{\vec{Q}}$ shows no interesting structure; the nesting function $\xi_{\vec{Q}}$ appears to be normally distributed. One possible explanation of the nature of the non-uniform distribution of matrix elements may be that the separate couplings come from the different nature of the electrons near the Fermi level. The shapes of the electronic eigenstates $\langle\vec{k}|$ and $\langle\vec{k}+\vec{Q}|$ and the overlap integral between them were analyzed for $\vec{k}$-s belonging to the stronger coupling peak and show little variance with pressure. Therefore the increase in matrix element strength appears to result from the complex interaction of the electronic states with the particular $T1$ phonon perturbation.

It is of interest to discuss the value of Coulomb pseudopotential we have used in Table I. Previously it has been suggested that higher values for μ^* are necessary to correctly describe Li.[16,34] The estimate of $\mu^*\approx 0.22$ was proposed

based on the comparison of Migdal-Eliashberg theory calculations of λ with McMillan equation based results for the superconducting transition temperature.[16] Before the superconductivity in Li was experimentally found, it had been proposed that the value of Coulomb pseudopotential for Li at ambient conditions should be greater that 0.1.[34] Additionally, it follows from the logic of Ref. 34 that pressure increases would decrease μ^*. However, we are not aware of any direct first-principles calculation of Coulomb parameter for Li, and specifically Li under pressure. Previous calculations on metals which exist in the literature provide values which are consistent with $\mu^*=0.13$ we employ.[35,36] Using this value a good agreement with the experimentally measured T_c is found. We have also included estimated T_c for $\mu^*=0.20$ for comparison in Table I.

The trend of the superconducting transition temperature increase of 1 K/GPa in the fcc phase in the 20–30 GPa region is promising for a higher temperature superconductor. Unfortunately, as the pressure is increased past 30 GPa, a complete softening of the $T1$ phonon branch along the Γ-K direction occurs. At this point the fcc crystal becomes unstable and likely transforms to the $hR1$ phase[9] preventing Li from reaching a higher T_c. We therefore offer a suggestion that by applying uniaxial stress along the same direction as the soft phonon eigenvector it may be possible to suppress the structural phase transition allowing for higher transition temperatures.

V. CONCLUSION

In conclusion, we investigated the origin of superconductivity in fcc lithium from first principles by considering the pressure evolution of the electron-phonon coupling parameter and its constituent elements. We found that superconductivity arises from pressure increased electron-phonon interaction and is highly affected by the topological features of the Fermi surface. We confirm that the lower transverse mode is responsible for over half of the coupling and specifically the phonon modes along Γ-K direction play the biggest role. We found that the electron-phonon matrix elements were the most sensitive to pressure of any contribution we examined. The matrix elements whose magnitudes depend strongly on the location in the BZ indicate a possibility of electron-phonon coupling arising from two distinct types of interactions having significantly different strengths. Our calculated superconducting transition temperatures as function of pressure are in good agreement with the available experimental data.

ACKNOWLEDGMENTS

This work was supported by National Science Foundation under Grant No. DMR07-05941 and by the Director, Office of Science, Office of Basic Energy Sciences, Division of Materials Sciences and Engineering Division, U.S. Department of Energy under Contract No. DE-AC02-05CH11231. Computational resources have been provided by the Lawrence Berkeley National Laboratory. Calculations were performed using the QUANTUM-ESPRESSO (Ref. 37), the WANNIER90 (Ref. 38), and the EPW packages (Ref. 39). T.B. thanks Jeffrey Neaton and James Schilling for useful discussions.

[1] E. Wigner and F. Seitz, Phys. Rev. **43**, 804 (1933).
[2] J. Tuoriniemi, K. Juntunen-Nurmilaukas, J. Uusvuori, E. Pentti, A. Salmela, and A. Sebedash, Nature (London) **447**, 187 (2007).
[3] M. Hanfland, K. Syassen, M. E. Christensen, and D. L. Novikov, Nature (London) **408**, 174 (2000).
[4] M. Hanfland, I. Loa, K. Syassen, U. Schwarz, and K. Takemura, Solid State Commun. **112**, 123 (1999).
[5] S. Deemyad and J. S. Schilling, Phys. Rev. Lett. **91**, 167001 (2003).
[6] V. V. Struzhkin, M. I. Eremets, W. Gan, H. Mao, and R. J. Hemley, Science **298**, 1213 (2002).
[7] K. Shimizu, H. Ishikawa, D. Takao, T. Yagi, and K. Amaya, Nature (London) **419**, 597 (2002).
[8] W. Schwarz and O. Blaschko, Phys. Rev. Lett. **65**, 3144 (1990).
[9] T. Matsuoka, S. Onoda, M. Kaneshige, Y. Nakamoto, K. Shimizu, T. Kagayama, and Y. Onishi, J. Phys.: Conf. Ser. **121**, 052003 (2008).
[10] T. Matsuoka and K. Shimizu, Nature (London) **458**, 186 (2009).
[11] V. E. Fortov, V. V. Yakushev, K. L. Kagan, I. V. Lomonosov, V. I. Postnov, and T. I. Yakusheva, JETP Lett. **70**, 628 (1999).
[12] P. B. Allen and M. L. Cohen, Phys. Rev. **187**, 525 (1969).
[13] A. Y. Liu, A. A. Quong, J. K. Freericks, E. J. Nicol, and E. C. Jones, Phys. Rev. B **59**, 4028 (1999).
[14] N. E. Christensen and D. L. Novikov, Phys. Rev. Lett. **86**, 1861 (2001).
[15] D. Kasinathan, J. Kunes, A. Lazicki, H. Rosner, C. S. Yoo, R. T. Scalettar, and W. E. Pickett, Phys. Rev. Lett. **96**, 047004 (2006).
[16] G. Profeta, C. Franchini, N. N. Lathiotakis, A. Floris, A. Sanna, M. A. L. Marques, M. Lüders, S. Massidda, E. K. U. Gross, and A. Continenza, Phys. Rev. Lett. **96**, 047003 (2006).
[17] Y. Yao, J. S. Tse, K. Tanaka, F. Marsiglio, and Y. Ma, Phys. Rev. B **79**, 054524 (2009).
[18] D. Kasinathan, K. Koepernik, J. Kunes, H. Rosner, and W. E. Pickett, Physica C **460-462**, 133 (2007).
[19] J. Neaton and N. Ashcroft, Nature (London) **400**, 141 (1999).
[20] P. B. Allen and R. C. Dynes, Phys. Rev. B **12**, 905 (1975).
[21] P. B. Allen and B. Mitrovic, in *Solid State Physics*, edited by H. Ehrenreich, F. Seitz, and D. Turnbull, (Academic, New York, 1982), Vol. 32, p. 1.
[22] G. Grimvall, *The Electron-Phonon Interaction in Metals* (North-Holland, New York, 1981).
[23] P. B. Allen, in *Dynamical Properties of Solids*, edited by G. K. Horton and A. A. Maradudin (North-Holland, Amsterdam, 1980), Vol. 3, p. 95.
[24] D. M. Ceperley and B. J. Alder, Phys. Rev. Lett. **45**, 566 (1980).
[25] J. P. Perdew and A. Zunger, Phys. Rev. B **23**, 5048 (1981).

[26] J. Ihm, A. Zunger, and M. L. Cohen, J. Phys. C **12**, 4409 (1979).
[27] N. Troullier and J. L. Martins, Phys. Rev. B **43**, 1993 (1991).
[28] S. Baroni, S. de Gironcoli, A. Dal Corso, and P. Gianozzi, Rev. Mod. Phys. **73**, 515 (2001).
[29] F. Giustino, M. L. Cohen, and S. G. Louie, Phys. Rev. B **76**, 165108 (2007).
[30] N. Marzari and D. Vanderbilt, Phys. Rev. B **56**, 12847 (1997).
[31] I. Souza, N. Marzari, and D. Vanderbilt, Phys. Rev. B **65**, 035109 (2001).
[32] F. Giustino, Jonathan R. Yates, I. Souza, M. L. Cohen, and G. Louie, Phys. Rev. Lett. **98**, 047005 (2007).
[33] L. Shi and D. A. Papaconstantopoulos, Phys. Rev. B **73**, 184516 (2006).
[34] C. F. Richardson and N. W. Ashcroft, Phys. Rev. B **55**, 15130 (1997).
[35] K. H. Lee and K. J. Chang, Phys. Rev. B **54**, 1419 (1996).
[36] Y. G. Jin, K. H. Lee, and K. J. Chang, J. Phys.: Condens. Matter **9**, 6351 (1997).
[37] S. Baroni, A. D. Corso, S. de Gironcoli, and P. Gianozzi, http://www.pwscf.org/
[38] A. A. Mostofi, J. R. Yates, Y. S. Lee, I. Souza, D. Vanderbilt, and N. Marzari, Comput. Phys. Commun. **178**, 685 (2008).
[39] J. Noffsinger, F. Giustino, B. Malone, C. Park, S. Louie, and M. Cohen, Comput. Phys. Commun. **181**, 2140 (2010).